

Precision Measurement of the Magnetic Moment of the Muon*

K. M. Crowe

Lawrence Berkeley Laboratory, University of California, Berkeley, California 94720

and

J. F. Hague,† J. E. Rothberg, A. Schenck,‡ D. L. Williams, R. W. Williams, and K. K. Young
Physics Department, University of Washington, Seattle, Washington 98105

(Received 22 November 1971)

A determination of the ratio of the muon to the proton magnetic moment, μ_μ/μ_p , is described. The precession rate of positive muons was compared to that of protons in the same magnetic field and chemical environment. Attention is given to the points which bear on the accuracy of the result: timing, magnetic field, many systematic checks, and particularly the question of the chemical environment of the μ^+ . It is shown experimentally that the so-called "Ruderman correction"—the ionic state in water once tentatively proposed by Ruderman—does not occur. A physical effect which excludes the possibility of the ionic state is pointed out. Consistent results were obtained in three different media: water, NaOH solution, and an organic liquid. Chemical corrections were ≤ 2 ppm. The result, including residual uncertainties in the chemical corrections, is $\mu_\mu/\mu_p = 3.1833467 \pm 0.0000082$ (2.6 ppm); in terms of the muon mass this implies $m_\mu/m_e = 206.7682 \pm 0.0005$, or $m_\mu = 105.6594 \pm 0.0004$ MeV. The new value for the muon moment, used with the most recent measurements of the muonium hyperfine interval, yields a value for the fine-structure constant of $\alpha^{-1} = 137.03632 \pm 0.00019$, an accuracy comparable with that of the current recommended value which depends primarily on the Josephson effect. The two numbers differ by 2.2 ppm, while the standard deviation of the difference is 2.1 ppm, which is satisfactory agreement.

I. INTRODUCTION

This paper describes a measurement of the magnetic moment of the positive muon, or more exactly the ratio of the muon moment to the proton moment, μ_μ/μ_p . Preliminary results have been reported¹; we give here some details relevant to the claim of high precision, especially a discussion of our knowledge of the chemical state, and "chemical shift," of the muon (Sec. V). The data and corrections have been thoroughly reworked since the publication of Ref. 1. The result is $\mu_\mu/\mu_p = (g/m)_\mu/(g/m)_p = 3.1833467(82)$, where (82) is the standard deviation in the last place. It is unchanged, apart from a slight shrinkage of the error, from the result of Ref. 1.

The two quantities μ_μ/μ_p and the " $g-2$ " frequency,

$$\omega_{g-2} = \frac{g-2}{2} \left(\frac{eB}{mc} \right),$$

are both needed to extract the muon's magnetic anomaly, $a \equiv (g-2)/2$, from a $g-2$ experiment. The current value² for a has an error of 270 parts per million (ppm), while the value of $(g/m)_\mu$ is far more precise, so the latter measurement has been relatively neglected. However, there is good prospect for a $g-2$ measurement with extremely good accuracy,³ so one will hopefully need μ_μ/μ_p to

better than the approximately 15-ppm uncertainty which it had from 1963 to 1970.⁴⁻⁶

Of more immediate interest is the relation⁷ between μ_μ/μ_p , the muonium hyperfine interval ν_m , and the fine-structure constant α :

$$\nu_m = \frac{16}{3} \alpha^2 \left(\frac{\mu_\mu}{\mu_p} \right) \left(\frac{\mu_p}{\mu_B} \right) R_\infty c (1 + \text{corrections}), \quad (1)$$

where the rydberg and the proton moment in terms of the Bohr magneton have errors well under a part per million. "Corrections" include recoil effects, the a value of the electron, and ~200 ppm of radiative corrections. Historically the Columbia value⁴ for μ_μ/μ_p and this relation were used when the first results for ν_m became available⁸ to obtain a value for α^{-1} which was 20 ppm above the value now considered correct. The subsequent search for the inconsistency led Ruderman⁶ to point to ambiguities in the chemical shift appropriate to the Columbia measurement. In the present work we show that Ruderman's speculation does not apply and that the chemical shift is relatively well known. Our results, combined with the most recent ν_m values (which differ from those of Ref. 8 by ~30 ppm) lead to a value for α which is in agreement to ~2 ppm with the value derived primarily from the ac Josephson effect.

The μ_μ/μ_p ratio can also be used to give a new value for the muon-electron mass ratio, m_μ/m_e

=206.7682(5). A new value for the muon lifetime will be discussed in a subsequent publication.⁹

II. EXPERIMENTAL METHOD

The standard method^{4,5} for measuring the magnetic moment of the muon has been to observe the precession frequency $geB/2mc$ of the muon at rest in a liquid, using the fact that the $(1+A \cos\theta)$ decay pattern rotates with the muon spin. In the present experiment, we followed this procedure. The statistical accuracy of the total data was 1.35 ppm; our aim was to get the systematic uncertainties down to this level. In this paper we emphasize those aspects of the experiment which were crucial to this aim.

A. Muon Beam and Target Setup

A highly polarized low-momentum beam of positive muons was obtained from a copper target in the external proton beam of the LBL 184-in. cyclotron. The method of Swanson *et al.*¹⁰ was used, making a momentum-selected pion beam with the first bending magnet, "Electra" in Fig. 1, then selecting a higher-momentum band with the second bending magnet, "Titan." The higher-momentum

particles are predominantly muons from forward decay of pions, and therefore well polarized. The polarization of the stopped-muon sample, as inferred from the observed asymmetry, was greater than 80%. In the stopping target (a $3 \times 3 \times 3$ -in. cube) we had typically 2000 muons per second.

Figure 2 shows schematically the counter arrangement around the stopping target. The probability of a decay-electron count in either of the electron counters E1 or E2 depends on the muon spin direction and therefore is modulated as the muon precesses. The amplitude A of the modulation (often called the asymmetry) will be reduced if the solid angle subtended by the counter is too large; hence two counters, mixed with a suitable delay in one of them, are better than one. The error in the angular frequency of the modulation, if N decay electrons are recorded over a time long compared to the muon lifetime τ , is essentially

$$\frac{\sigma_\omega}{\omega} = \frac{\sqrt{2}}{\omega\tau A\sqrt{N}}. \quad (2)$$

An important criterion, therefore, is to keep A as large as possible (see also discussion of timing below). Another criterion is that all electrons should come from the target, rather than from

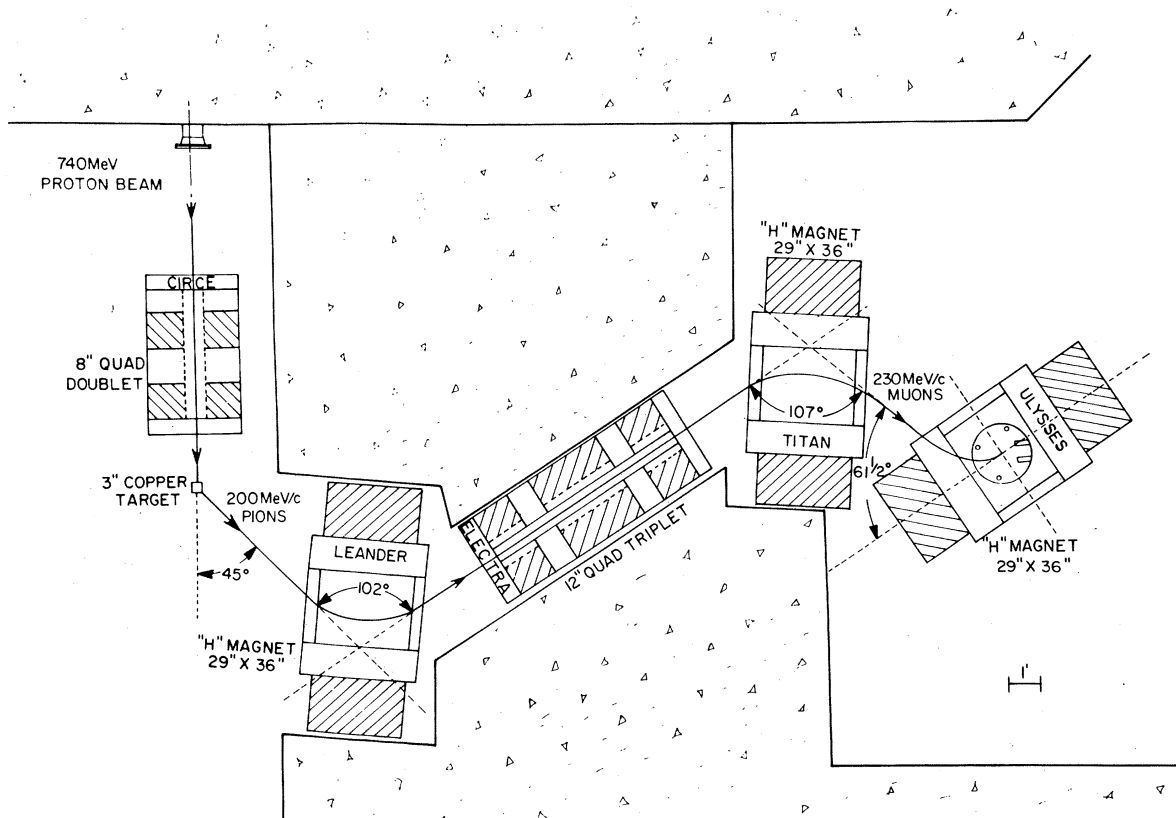


FIG. 1. Beam arrangement (plan view).

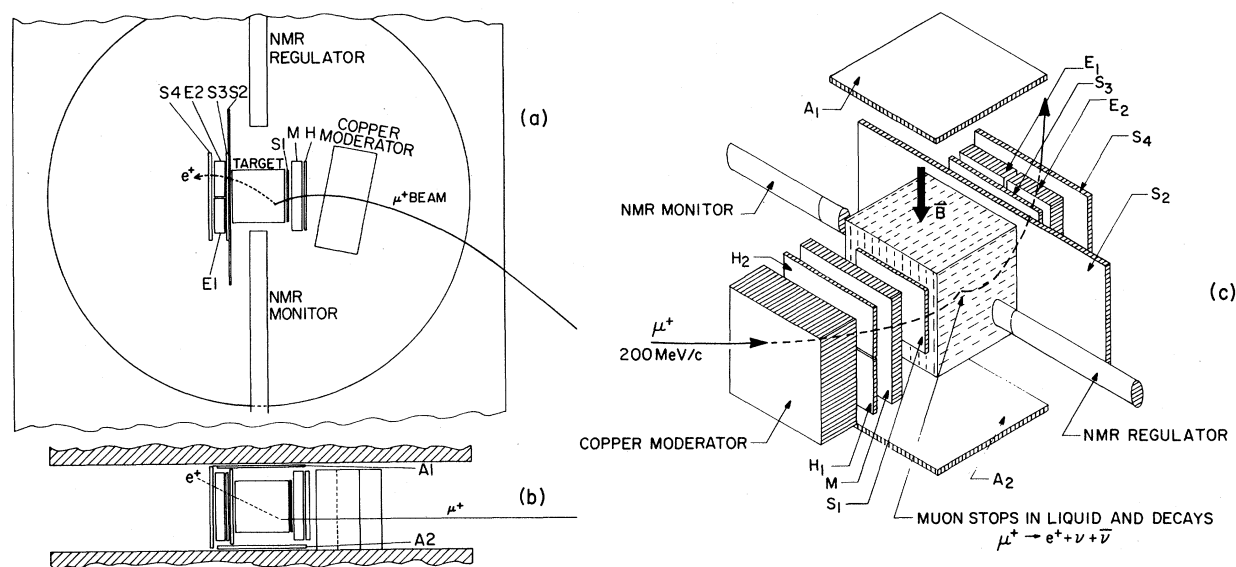


FIG. 2. Experimental arrangement. The target is $3 \times 3 \times 3$ in. (a) Plan view; (b) elevation (NMR probes removed); (c) exploded isometric view. The target and the counters are set between the precision magnet pole faces. The stopping muon is (beam) $\cdot (H \cdot M \cdot S1) \cdot [\text{not}(S2 + A1 + A2)]$. The signal for the decay positron is $S3 \cdot (E1 + E2) \cdot S4 \cdot [\text{not}(S1 + A1 + A2 + M)]$.

pole pieces, counter wrappings, etc. To this end the counters were highly efficient, thinly wrapped, and thin if necessary. The upper and lower anticoincidence counters $A1$ and $A2$ and the large prompt anticounter $S2$ were essential in reducing background. The defining counters $S1$, $S3$, $S4$ played roles defined by the two logic signals¹¹:

$$\text{Muon} = (\text{Beam}) \cdot (H \cdot M \cdot S1) \cdot [\text{not}(S2 + A1 + A2)],$$

$$\text{Electron} = S3 \cdot (E1 + E2) \cdot S4 \cdot [\text{not}(S1 + A1 + A2 + M)].$$

For good time resolution the timing counters M , $E1$, and $E2$ were made of thick fast plastic (1.25 cm of NE111), coupled to Amperex XP-1021 phototubes.

One incident counter, H , was divided horizontally so that the two halves could be monitored separately by the hodoscope (Sec. IID). Stability of the

$H1$ - $H2$ ratio, and the $E1$ - $E2$ ratio, also monitored by the hodoscope, assured us that the beam did not shift.

The target substances were water, sodium hydroxide solutions, and an organic liquid, methylene cyanide (or malononitrile), $\text{CH}_2(\text{CN})_2$. These were contained in 3-in. cubic boxes of 5-mil Mylar. Rates, background contributions, etc., are collected in Table I.

B. Timing

Since accuracy is inversely proportional to frequency, or magnetic field [Eq. (2)], the field should be as high as is consistent with uniformity requirements (Sec. III) and with the electronic timing. Time resolution, like spatial resolution, decreases the effective asymmetry A . Our problem was to

TABLE I. Rates and background contributions.

Stopping volume	$3 \times 3 \times 3$ in.	(Liquids in Mylar)
Container contribution		1%
Target-out rate		$2\frac{1}{2}\%$
Background rate		1% of early channels
Space variation of magnetic field over stopping volume		2.2 ppm (rms)
(Weighted-average field) - (field at center)		0.1-0.4 ppm
(Field at monitor position) - (field at center)		3 ppm
Timing resolution		0.6 nsec FWHM
Least count, fully digital system		1.25 nsec
Least count, digital-plus-analog interpolation		0.5 nsec
Decay-electron rate		60/sec
Asymmetry in H_2O		0.16

record the interval between muon arrival and electron arrival with complete linearity and with resolution good compared to $2\pi/\omega$. Good timing was achieved by the two-discriminator method: The pulse height of the outputs of the timing counters was required to be >400 mV, while the fast-timing discriminators (EG & G type T200/N) were set at 100-mV threshold. The resolution measured for straight-through particles was 0.6 nsec full width at half maximum (FWHM); there is indirect evidence that the timing of the μ - e sequence was comparably good.¹²

The μ - e interval must be measured on a scale which is linear in a part-per-million sense; comparison with a crystal-controlled frequency was the only available principle to accomplish this. Unlike the previous experiments^{4,5} we measured time directly, in terms of the period and number of cycles of a free-running oscillator. The essential element is a scalar which can be gated on by the start (muon) pulse, and off by the stop (electron) pulse. Such a device has been used in a number of muon experiments^{2,13} and is often called a digitron. Our system was unusual in two respects: (a) The digitron was actually double with two entirely independent systems running from one "clock" (crystal-controlled cw signal). This not only provides checks on the system but allows an effective doubling of the time resolution, as explained below. (b) A completely separate commercially made system, using a slower crystal clock and analog interpolation, was used and recorded at the same

time as the digitrons. This system is called by the manufacturer, Hewlett-Packard, a type 5360A Computing Counter. The two digitrons were compared on an event-by-event basis; the muon frequency they determined was compared with that from the HP counter, as explained in Sec. IV.

The heart of the digitrons was a pair of fast-gated high-speed prescalers developed by the Physics Instrumentation Group at the Lawrence Radiation Laboratory; they have been described¹⁴ by their designer, K. Lee. They can operate at frequencies up to 495 MHz, but were used by us at 400 MHz. Reference to the block diagram, Fig. 3, shows that the clock is continuously present at the input of both prescalers. The timing signal from the muon opens the control gate; the timing signal from the electron activates the stop gate which closes the control gate in synchronism with the clock train.¹⁵ It is easy to show that the number of clock pulses recorded, times the clock period τ_c , gives an unbiased estimate of the time interval, while the effective resolution function is triangular with a base equal to twice the period.

The period of muon precession frequency was about 7 nsec, so the resolution of a single digitron caused some reduction in the modulation amplitude A of the precession curve. It was our hope — which proved justified — that digitron operation would be so stable that we could effectively double the frequency, operating the two digitrons in a mode we call "split," with the clock signal to one exactly 180° out of phase with the signal to the other. Each

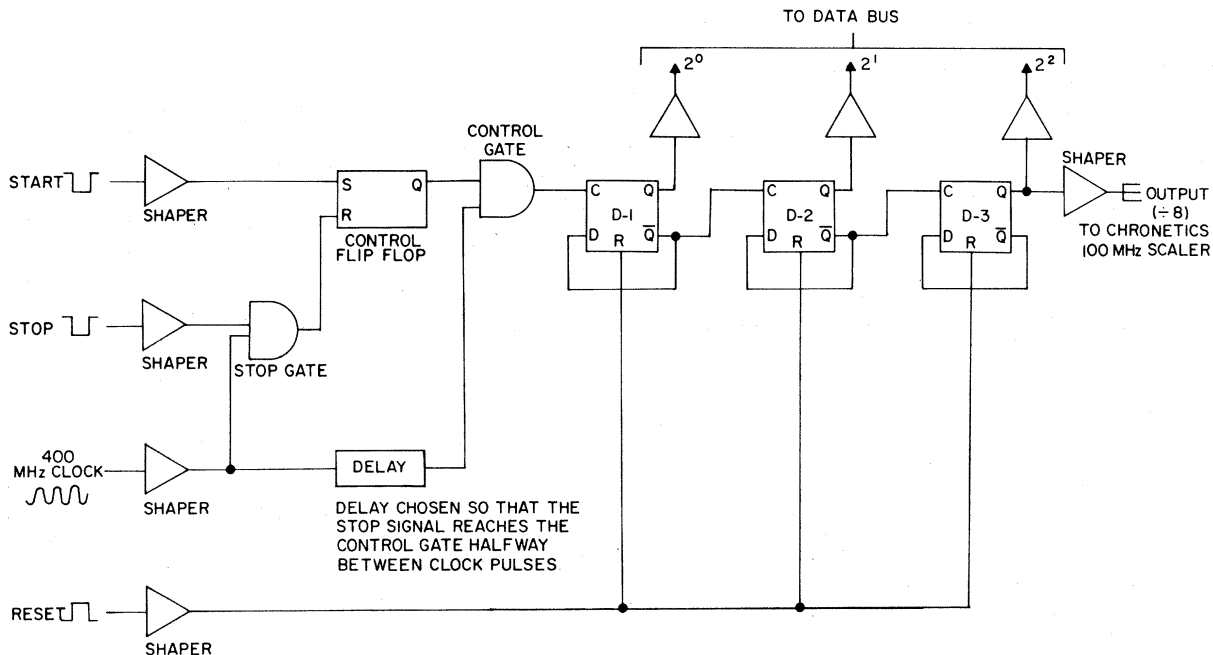


FIG. 3. Simplified schematic of the 400-MHz prescaler used in the digital timing system.

event generated two numbers, n_1 and n_2 , which should not differ by more than one unit. The elapsed time for that event was $(n_1+n_2)\tau_c/2$. We have the equivalent of a single digitron of least count $\tau_c/2 = 1.25$ nsec, plus the internal checks afforded by recording n_1 and n_2 separately.

The HP Type 5360A counter was a multipurpose device, used in its interval-measuring mode. The time base was provided by an internal crystal-generated 10-MHz frequency. The start and stop times were interpolated, within the 100-nsec least count, by an analog device which was then converted to digital information using the same clock. Long-range linearity was thus assured, and the local nonlinearity proved to be very small. The device was set for a 0.1-nsec least count. The dead-time of the device was rather long. It was therefore operated in a time-inverted mode in which the muon pulse was stored in a long recirculating delay cable. If the logic then indicated a good event, the HP counter was started by the electron signal, and stopped by the muon signal.

The digitrons were subjected to numerous bench tests, including: Checking them against each other when they were set for 0° phase difference; generating random time intervals using a radioactive source, and observing the uniformity of response; observing the sensitivity to variation of clock-signal amplitude. The only effects which can lead to a wrong value for the frequency are those which depend on the elapsed time between start and stop. Thus, for instance, timing errors associated with discriminator level shifts, etc., will reduce the modulation amplitude of the data but will not cause any error in the frequency.

Another type of elapsed-time error can occur if the electron channel has a recovery-time effect (e.g., baseline shift) in it, and a signal occurs in the electron channel before a muon signal occurs. Measurements indicated the recovery time of our system to be tens of nanoseconds; nevertheless we flagged, by means of a hodoscope bit, those events for which the electron line had a signal at any time during the $1 \mu\text{sec}$ preceding a muon signal; these events were later removed.

The HP counter was recorded separately from the digitron, so that it yielded an independent final result. It is gratifying that the final frequency result of the experiment is the same (differing by only 0.3 ppm) whether compiled from the digitron results or the HP counter results.

On-line tests and off-line software tests will be described in Sec. IV.

C. Magnet

A window-frame magnet with 29×36 -in. poles was fitted with a special precision-ground 24-in.-

diam pole-tip assembly. This assembly, which included several sets of correction coils, was designed by G. McD. Bingham and used by him in a previous measurement.⁵ In preparing the uniform magnetic field we followed the procedure he describes,¹⁶ with the addition of a few small pieces of 0.001-in. steel for final shimming. Over the $3 \times 3 \times 3$ -in. target volume the final field had a uniformity of about 2 ppm (rms) at 11 000 G. The field strength chosen was a compromise between the advantages of high frequency [Eq. (2)], the concomitant reduction in A if the time resolution becomes dominant, and the adverse effects of saturation on field uniformity. This field corresponded to about 149 MHz for muons and 46.8 MHz for protons.

D. Frequency Generation and Measurement

The experiment was digital and essentially automatic, under the control of a small on-line computer (DEC PDP-5). Each event consisted of three timing numbers – the two digitrons and the HP counter – and the information bits which recorded the presence of a count in $H1$, $H2$, $E1$, and/or $E2$, the presence of an early (before the muon) electron count, a second “muon” in the 20- μsec event gate, or a second “electron.” To monitor the two time bases of the experiment – the 400-MHz clock and the frequency of proton precession in the field – we used two Hewlett-Packard crystal-controlled frequency counters, type 5245L (these counters had a least count of 10 Hz; the 400 MHz was demultiplied with a type 5253B plug-in). Monitoring frequencies to 1 in 10^7 presents no problems, but it was the pleasure of the experimenters to hook the two counters to the same crystal, so the basic crystal frequency would cancel out. The 400-MHz signal was obtained from a Hewlett-Packard type 608F Signal Generator in conjunction with a Hewlett-Packard type 8708A Synchronizer. The frequency was highly stable, so that the continuous check was superfluous. The clock in the HP counter was also checked against our other frequency standards.

E. Data Recording

The digital information of each event was stored in the memory of the PDP-5. When this buffer was full (142 events) the contents were transferred to magnetic tape, along with the contents of the two frequency counters at that point. No editing was done by the on-line computer.

III. MAGNETIC FIELD

A. Regulation

The field regulation had to correct for fast fluctuations of the current from the main power supply

(stable to $\sim 10^{-4}$) and for slow variations and shifts due both to the power supply and to changes of the magnetization of the magnet poles. Regulation was accomplished by passing current through a pair of correction coils around the pole tips. The fast-change correction signal came from the voltage at a pair of pick-up coils, while the basic stabilization was provided by a proton NMR probe.

The slow variations and shifts were stabilized to better than 1.5 ppm, and also monitored by an independent system. The block diagram of the regulation system is given in Fig. 4. The probe circuit is tuned to act nearly as a $50\text{-}\Omega$ terminator at its resonance frequency, which is close to the external driving frequency $f_0 = 46.80000$ MHz (from a Rhode and Schwartz generator, which was stable to better than 10^{-8}). The NMR signal was detected via a change of the impedance of the circuit and consequently by a change of reflected rf power from the circuit. The complex inductance of the circuit is given by $L = L_0(1 + 4\pi\chi)$, with $\chi' + i\chi''$ the dynamical susceptibility which arises near the resonance condition for the protons. For fixed driving frequency f_0 , χ'' has a Lorentzian dependence on the field B_0 , while χ' has a dispersionlike B_0 curve. If the probe circuit is tuned far enough off resonance one finds

that the reflected power depends to good approximation on χ' alone. We found this tuning more stable against thermal and mechanical changes than on-resonance tuning, and we used it for both the regulation system and the field monitor.

By modulating the static magnetic field at the probe with a frequency of 22 Hz and a sweep width of 20 mG and using conventional lock-in technique we recorded the derivative of the NMR signal. The NMR signal for regulation was obtained from a small cylinder (diameter 4.4 mm, length 10 mm) filled with 0.05 M $\text{Fe}(\text{NO}_3)_3$ solution.

The regulation was accomplished by using the output signal of the lock-in amplifier to drive the correction-coil current source. In this way the magnetic field was locked to a value which corresponds to a zero crossing of the derivative of the NMR signal.

B. Field Measurement and Monitoring

The magnetic field was monitored by an independent proton-magnetic-resonance setup. The block diagram is given in Fig. 5. The integrated output signal of the lock-in amplifier was used to feed a HP-8708A synchronizer (crystal controlled) which

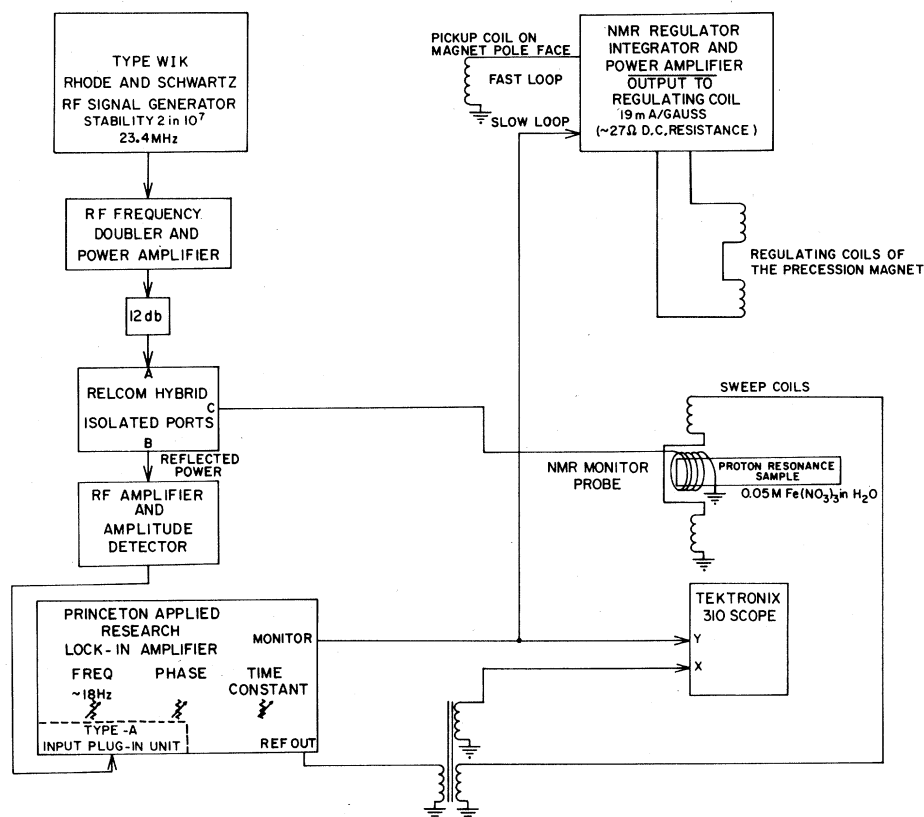


FIG. 4. Schematic of the NMR regulator system.

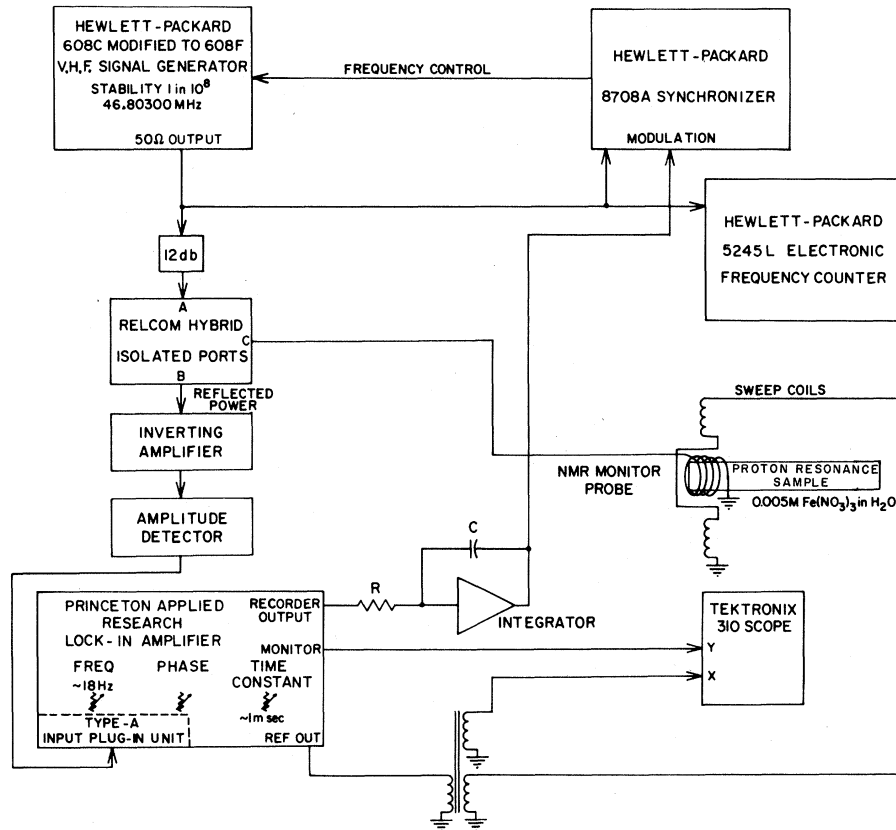


FIG. 5. Schematic of the NMR monitoring system.

forced the frequency of the vhf generator (HP 608F) to be always at the value at which a zero crossing of the derivative of the NMR signal occurred. The generator frequency was measured by one of the frequency counters referred to above. The observed linewidth (between zero crossings) was about 200 Hz, which corresponds to 4 ppm of the resonance frequency (or the field).

The position of the two probes during normal running is shown in Fig. 2. The field (frequency) at the center of the target, f_c , was measured every two hours during the course of a run by removing the target and inserting the monitor probe into the magnet. The probe holder provided click-stops to achieve accurate and reproducible positioning of the probe. The frequencies of both zero crossings of the derivative of the NMR dispersion signal were measured and averaged to obtain f_c , Fig. 6. Similar measurements were made with the probe in the monitor position to obtain a value for f_m . The difference, $\Delta = f_c - f_m$, was usually about 150 Hz, and never changed by more than ± 40 Hz (0.8 ppm) during a run. The line width, δ , was determined from these measurements to ≈ 0.7 ppm. The average field at the center of the target, f_c^{av} , is given by

$$f_c^{av} = f_m^{av} + \frac{1}{2}\delta + \Delta, \quad (3)$$

assuming a symmetric line.

To check the symmetry of the line shape the line was traced out by plotter on a number of occasions; the result was always that the asymmetry was so small as to cause negligible (< 0.1 ppm) error. The signal-to-noise ratio was $> 50:1$.

C. Average Field and Corrections

The value for the proton resonance frequency (or the field) at the center of the target is of course not necessarily identical with the field average over the target volume. The field average must

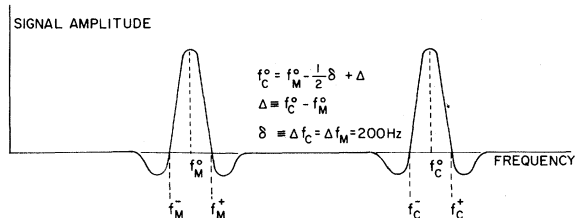


FIG. 6. Definition of the frequencies entering in the magnetic field measurement.

reflect the stopping distribution of the muons, suitably weighted by the counting efficiency and decay asymmetry over the target volume.

Three field maps were made during the course of the experiment by moving the monitor probe through its range of locking positions in three dimensions. Both zero-crossing frequencies were recorded at 343 positions over a volume of $6.7 \times 9.5 \times 9.5$ cm. The rms deviation of the field over the target volume was <2.5 ppm. To determine the muon stopping distribution, a target, the same shape as the standard liquid target, was constructed from 27 2.54-cm cubes of polyethylene which has about the same stopping power as water. The stopping rate was measured in each cube for the same number of incident beam particles. The method was to add to the normal logic requirements the condition, in the "stop" signal, $C1 \cdot [not(C2)]$, where $C1$ is a small counter just ahead of the block in question, and $C2$ a similar counter just behind the block. Thus we record electrons coming only from one cube, automatically obtaining the stopping-density-efficiency product for that cube. To measure the asymmetry of the signal we effectively summed over all cubes in a plane perpendicular to the beam. The results were $A(\text{upstream}) = 0.26$, $A(\text{center}) = 0.20$, $A(\text{downstream}) = 0.15$. The field average over the target volume was then obtained by weighting each field point by the product of asymmetry and normalized counting rate and calculating the average.

The difference of the weighted field average from the value at the center of the target is given in Table II for the different field maps. Table II shows also the rms deviation of the field from the weighted average. The field was so uniform that no combination of field map and weighting shifted the result more than ± 0.2 ppm. The final value for the average proton Larmor precession frequency was then calculated as follows: $f_p = \bar{f}_c + 0.27$ ppm. The uncertainty, primarily due to fluctuations in the difference between \bar{f}_c and f_m , is assigned to be ± 0.8 ppm.

The volume susceptibility of the liquids used was about -0.7×10^{-6} . The diamagnetic weakening of the field in the probe (a cylinder) will be slightly different from that in the target (a cube). We have calculated numerically the average shielding factor for a cube (about 1% different from a sphere), and find that the field in the cube is weaker, by 1.5 ppm, for both target materials used. (In NMR spectroscopy this is called the bulk susceptibility correction. It is $\frac{2}{3}\pi\chi_v$ for the sphere-cylinder comparison.)

The time variation of the field at the monitor was recorded with every data transfer, several times a minute; the rms variation was <1.2 ppm, and the

TABLE II. Results of averaging magnetic field over stopping distribution, for three field maps.

No.	$\Delta\bar{B} = B_{av} - B_c$	ΔB_{rms}
1	+17 Hz (+0.36 ppm)	99 Hz (2.1 ppm)
2	+17 Hz (+0.36 ppm)	133 Hz (2.8 ppm)
3	4.1 Hz (+0.09 ppm)	76 Hz (1.6 ppm)
Average	+0.27 ppm	2.2 ppm

correct time average was used in Eq. (3).

A number of small effects which could lead to field errors were investigated. Among these were:

(1) Sample purity. The probe solutions and the various target materials were all run on the Varian 60 high-resolution NMR system in the University of Washington Chemistry Department. The frequencies were as expected; the chemical shifts used in Sec. V are based on these measurements.

(2) Magnetic dirt. The probe assemblies were checked for paramagnetic materials, and the Mylar target box was checked for ferromagnetic dust.

(3) Effect of scintillators and shields. The counters and their shields were always in place when measurements were made.

(4) Loss of lock in either monitor or stabilizer loop. Software eliminated such data after at most 30 sec of trouble.

(5) Sample-stabilizer probe interaction. When the sample is in place its diamagnetism causes a little flux to be pushed away from the center, increasing the field at the stabilizer probe. Removing the sample (for the measurement of f_c) should thus cause the stabilizer to call for more magnet current. Calculation and measurement indicated that this subtle error was negligible.

IV. DATA REDUCTION AND ANALYSIS

Data analysis progressed in five phases. In the first phase checks were made on the data by use of the on-line computer which was recording events on magnetic tape; all data were transferred to tape. Results were presented in the form of type-written messages and oscilloscope displays, to check on operation of the experiment. The second phase was the generation of a histogram tape of selected events vs time from the raw data tapes; and the third was a maximum-likelihood computer fit of the histogrammed events to obtain the best estimates of the fitted parameters. The resulting values for the muon precession frequency were then combined with magnetic field data to obtain uncorrected values for the ratio ω_μ/ω_p . In the fifth and last phase of analysis, corrections were made for systematic effects and these results were combined to yield the final value for the magnetic moment ratio.

The on-line computer checks were invaluable in correcting faults in the equipment, but were not essential to the data analysis, so they will not be described further.

A. Editing and Filtering the Data

Upon completion of a data-taking run, the data tape was processed by an editing program which made tests, performed the filtering described below, and generated time histograms on magnetic tape as the end result. The histogram tapes were later analyzed to determine the best values of the fitted parameters by the maximum likelihood method. Each data tape was read four times and four histograms were written on the output tape: 8000-bin histograms (2.5 nsec per bin) of Digitron-1 and Digitron-2, a 16000-bin histogram (1.25 nsec per bin) of the sum of $D1$ and $D2$, called the "split digitron," and a 20000-bin histogram (0.5 nsec per bin) for the HP computing counter.

Filtering criteria were of three types, (1) general bookkeeping: run number correct, etc.; (2) magnetic field check: NMR monitor probe's most recent value to be within 1 kHz of the preset standard; (3) event-by-event check to accept only clean events. The latter included what is sometimes called "confusion elimination," elimination of events which have more than one electron within the data gate. With background counts present (in our case they constituted 1% of the early counting rate) the distribution of the interval between muon and first electron will have the form "exponential plus constant" only if second-electron events are removed, otherwise the background will itself have a small exponential slope. This is crucial for obtaining the correct muon lifetime, but has only higher-order effects on the precession-frequency measurement.

Type-(3) criteria were applied as follows: The hodoscope was tested and tallies were kept of the bits which were set. Events which had second muon or second electron signals within the 20- μ sec data gate were rejected as well as those which had a pulse in an electron counter up to 1 μ sec prior to the arrival of the stopping muon signal. Events for which more than one H counter or more than one E counter counted were also rejected. The digitrons' values were acceptable if the absolute value of their difference was one or zero, since Digitron-1 was phase shifted by one-half of a clock cycle behind Digitron-2; and this phasing scheme caused bin n of Digitron-1 to overlap bins n and $n+1$ of Digitron-2. The Split-Digitron value was taken to be the sum of Digitron-1 and Digitron-2; there was no check for agreement between the Split-Digitron and the Hewlett-Packard Counter.

The contents of the timing device being processed became the histogram's bin address which was incremented by one. Table III summarizes some rejection rates from the hodoscope filter.

When all of the timing data had been processed, the average value of the magnetic field at the monitor probe position and its rms deviation were calculated, and a summary of information for that data tape was printed.

B. Maximum-Likelihood Fit to the Data

The fitting program was used to determine the parameters N , A , ω , ϕ , B which describe the arrival rate of electron counts according to the formula

$$N(t) = N\{[1 + A \cos(\omega t + \phi)] \exp(-t/T) + B\}. \quad (4)$$

The muon lifetime, T , was usually taken to be the currently accepted value of 2.198 μ sec, but it could be left as a free parameter and included in the fit. The values of the fitted parameters were determined by the maximum-likelihood method using Poisson statistics to describe the distribution of counts in each histogram channel. The program also determined the error matrix by numerical approximation to the second partial derivatives of the likelihood function.

The fitting program was based on an efficient multiparameter variable metric minimization program, VARMIT, available from the disc library of the Berkeley CDC-6600 system.

To ensure that the numerical approximation used in calculating the errors was operating correctly, the logarithm of the likelihood function was plotted versus frequency, allowing the correlated parameters to float free. The standard deviation as found from the $(\ln L_{\max} - \frac{1}{2})$ points agreed with that from the error matrix. The fitted parameters were used to calculate χ^2 for each run; typically the number of degrees of freedom was 7700 for the split digitron and the χ^2 value was within the statistical deviation expected.

C. The Combined Results

For each run (i.e., each data tape) the maximum-likelihood fit yields a value for the muon precession frequency and its standard deviation. We combined the data in two ways: run by run, obtaining local frequency ratios ω_μ/ω_p , then combining them with appropriate statistical weights; and data summing, in which a grand histogram containing millions of counts was made for each target material.¹⁷ The results agreed to 0.1 ppm. In comparing the results from the digitron with those from the HP counter (numerical results are given in Sec. VI)

TABLE III. Summary for a typical run.

(a) Processed events	
Number of events transferred	938448
Number of events passing NMR test	929602
Number of events passing phase check	929506
Number of events with no second μ , second e , or early E	832412
Number of events with [H_1 and (E_1 or E_2)] or [H_2 and (E_1 or E_2)]	689458
Number of events with digitron-1 and digitron-2 < 7952	689458
Number of events with $ D_2 - D_1 \leq 1$	689170
Number of events going into the histogram	689170
Digitron differences: ($D_2 - D_1$)	
-1	171550
0	344088
+1	173532
Average NMR monitor frequency (Hz)	46803630
rms deviation (Hz)	57.474
Number of tape records written	6596
(b) Information bits set by the hodoscope	
	Number of events
No second μ , no second e , no early E ^a	832412
Second μ only	84585
Second e only	5520
Second μ and second e	2601
Early E only	3812
Early E and second μ	524
Early E and second e	34
Early E and second μ and second e	18

^a $E = (E_1 + E_2)$ timing signal; $e = S_3 \cdot S_4 \cdot (E_1 + E_2) \cdot [\text{not } (S_1 + A_1 + A_2 + M)]$.

we did not expect precise agreement, even though the data are essentially the same: Different rejection criteria, and a different time resolution, do lead to a nonidentical data selection. We expect the differences to be a fraction of a standard deviation, and fortunately this is the case for the final result. Individual target materials showed differences of up to 1 standard deviation.

D. Tests of the Data

Most of the data were run through the analysis program many times, testing the stability of the results against a variety of changes. Among these were: various ways of combining the data; starting (or ending) the analysis interval at different times; changing the starting values or convergence criteria of the program; allowing the muon lifetime to float, or allowing the background to have an exponential decay. Nothing made any difference beyond the tiny fluctuations caused by different selections of data.

Extensive artificial data, generated by a simple Monte Carlo program, were also run through the analysis. Among the various effects investigated

were the effect of nonuniform background and the effect of odd-even alternation in the histogram. An artificial alternation of 10% [contrasted with the largest observed alternation of $(0.3 \pm 0.1)\%$] was tested in this way: The frequency did not change, within the error. The over-all conclusion was that the precession frequency is remarkably stable against dirt effects.

V. CHEMICAL ENVIRONMENT EFFECTS

The effect of an external magnetic field on a proton or muon which serves as a nucleus in a normal (i.e., diamagnetic) molecule is reduced by a fractional amount σ , generally 20–30 ppm, by the shielding of the atomic electrons. The exact amount varies by a few ppm for different chemical species, the variation being known as the chemical shift, δ . We measure the precession frequency of the muon in some molecule, compared to the frequency of the proton in water. To obtain the true ratio of muon to proton magnetic moment we must know the chemical shift of the muon, i.e., the fractional amount, δ , by which the muon frequency would be changed if the effective field at

the muon were exactly the same as that at the proton in water.¹⁸ This amount is not zero even for μHO , because of an isotope effect caused by the different zero-point energy. Muon moment measurements in liquids have been under a cloud since the suggestion by Ruderman⁶ that δ in water could be as large as 15 ppm. In this section we consider two problems: (1) the chemical state of the μ^+ during the precession measurement, and (2) the difference δ between the shielding of the μ^+ and the shielding of a proton in the H_2O comparison sample.

A. The Fate of Positive Muons Stopping in Gases or Liquids

Insights into this problem can be obtained from experiments done on protons stopping in matter. Figure 7, from the review by Allison and Garcia-Munoz,¹⁹ shows the charge state of a beam of low-energy protons losing energy in a gas, or, alternatively, emerging from an aluminum foil. As the velocity of the beam drops to $v \sim \alpha c$ (the "Bohr-radius" mean speed of an atomic electron in H) the often-discussed capture-and-loss regime sets in. As the velocity decreases, capture wins and the beam becomes progressively more neutral. At velocities of $\sim 0.002c$, corresponding to 200 eV for a muon, the beam becomes more than 90% neutralized. The reason is clear: Charge-exchange cross sections are large, and in the region $v < \alpha c$ the energy loss per collision is low enough that there are many collisions and quasiequilibrium is established. Thus the state of lowest energy predominates. Since the ionization potential of the hydrogen atom or the muonium atom (μ^+e^-) is

13.6 eV, and the ionization potential of nearly everything else is $\lesssim 10$ eV, the H (or muonium) is favored, except, of course, for slowing down in He, which has an ionization potential of 24 eV.

It is experimentally established²⁰ that μ^+ 's reach thermal energies as atoms rather than ions in argon and krypton, since muonium signals corresponding to essentially all the stopping muons are observed in these gases.

In this experiment the muons are stopped in water and in a substituted hydrocarbon. As the neutralized μ^+ (a muonium atom) approaches thermal energy in such media, what happens? Fortunately there have been detailed investigations of the analogous question for fast tritons and heavier radioactive ions, using the techniques of tracer chemistry. By several ingenious techniques it has been shown that in gases²¹ (excluding noble gases) the ^3H atom, as it slows down, either becomes part of a molecule in an energetic "hot-atom" collision, or reaches thermal energy as an atom. The usual picture of molecules, that the electronic and nuclear motions are well separated (the Born-Oppenheimer separation), leads to the near absence of isotope effects in chemistry. Isotopic effects in hot-atom reactions are not large, according to Wolfgang,²¹ and the quasiadiabatic picture applies to hot reactions better than a billiard-ball collision model does (the latter would have profound mass effects). Thus we can expect the muon, though 27 times less massive than the triton, to have qualitatively similar hot-atom chemistry and either to plunge into molecules in the several-eV region in which chemical reactions are favored, or to reach thermal energy as a muonium atom which rapidly depolarizes. Figure 8 illustrates the situation schematically. It is especially noteworthy that the hot-atom chemistry studies of tritium show that approximately half the tritium reaches thermal energy in atomic form; this explains the fact that μ^+ 's in media like water or most hydrocarbons show approximately 50% depolarization. Hot-atom chemistry in liquids has been less studied than in gases, but the qualitative features are the same.²¹

The objection raised by Ruderman⁶ to the Columbia measurement of the muon moment was that a μ^+ ion in water might, because of its low mass and the strongly hydrogen-bonded structure of water, find itself trapped as a metastable ion in a very unlocalized state, even though its thermodynamically stable state is μHO . As a metastable ion it would be relatively unshielded, perhaps 15 ppm less than in the molecule μHO , which has 26 ppm shielding. Of course this objection does not apply to the situation we have outlined above, in which the muon does not reach thermal energies as an ion. Never-

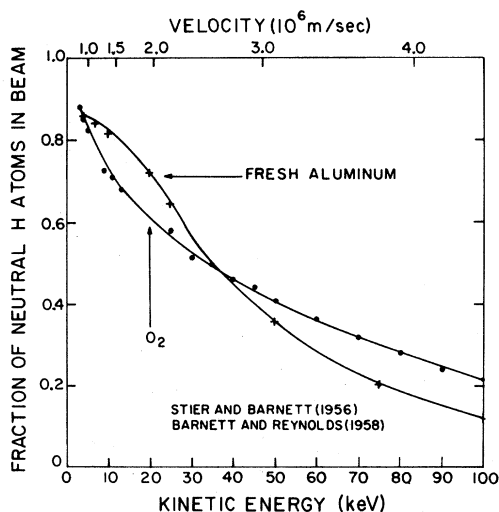


FIG. 7. Evidence that protons approach the end of their range as H atoms. The critical velocity is $\alpha c = 2.2 \times 10^6$ m/sec.

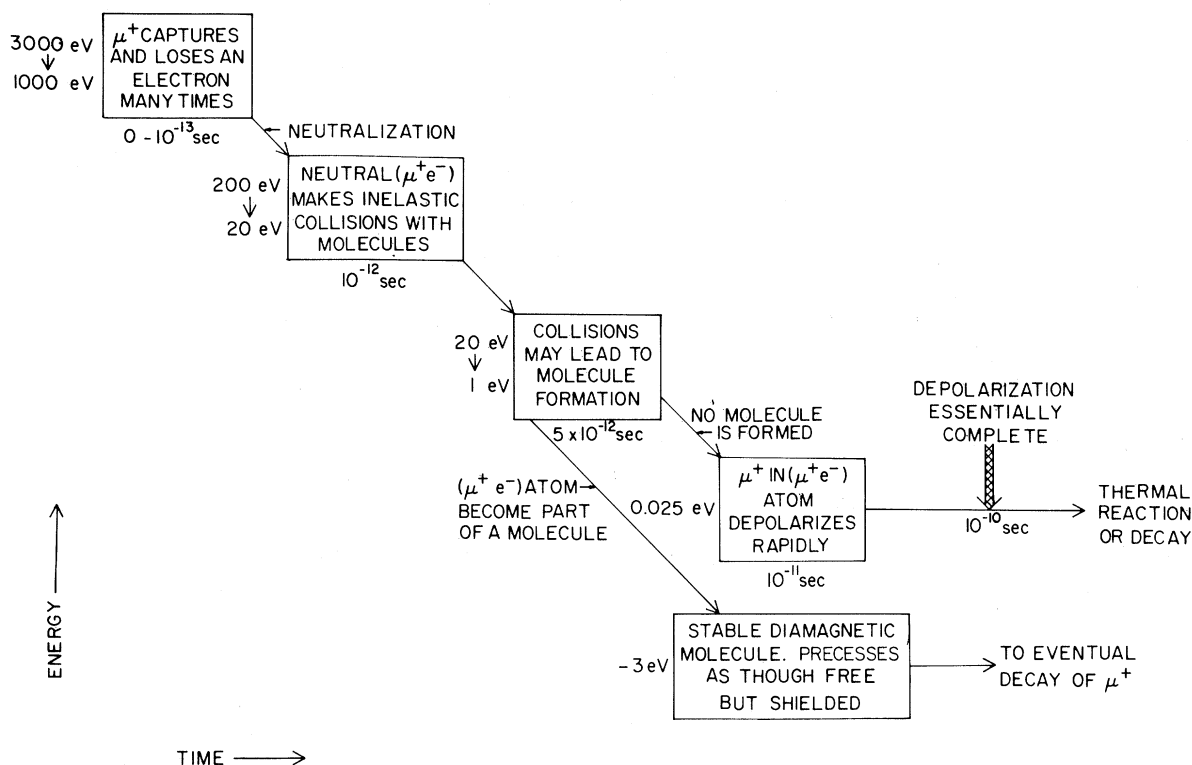


FIG. 8. Schematic history of a μ^+ in a gas or liquid, at energies below the electron-capture energy. In many liquids it appears that the upper (thermal muonium) branch and the lower (hot-atom) branch have comparable probabilities.

theless, our experiment was designed to detect the Ruderman effect, if it existed. We made use of the fact that chemical kineticists have, in recent times, succeeded in measuring the rates of neutralization reactions such as $H^+ + OH^- \rightarrow H_2O$ and $R^+ + OH^- \rightarrow ROH$ where R^+ might be, for example,²² an amino acid. These reactions, in aqueous solution, prove to be extremely fast, limited only by the rate at which the reactants approach one another, that is, by diffusion. The mean life of an R^+ ion in water containing (OH^-) ions in one normal concentration proves to be less than 10^{-10} sec. Any "Ruderman acid" [his proposed form was $(H_2O - \mu - H_2O)^+$] would be neutralized, in 0.1 *N* NaOH solution, in a time very short compared to the muon lifetime.

The experiment was carried out in distilled water and in NaOH solutions. If Ruderman's mechanism were operating the latter should have a frequency ~ 15 ppm lower than the former. In addition, we used as a stopping material $CH_2(CH)_2$, an organic liquid (it freezes at $31^\circ C$) which, since it is not hydrogen-bonded, avoids the complications introduced by water. This particular substance was chosen because it easily forms negative ions, $(CN)_2CH^-$, which would react with any μ^+ ions which happened to be present, just as OH^- would in water. (In retrospect this was an unimportant consideration, since muons do not stop as ions.)

The negative ions were formed²³ by adding 0.02 moles per liter of solid KOH, which dissolved to give $CH_2(CN)_2 + KOH \rightarrow (CN)_2CH^- + K^+ + H_2O$.

Table IV gives the ratio of muon precession frequency to proton precession frequency, ω_μ/ω_p , for distilled water,²⁴ 0.1 *N* NaOH solution, and 0.5 *N* NaOH solution. The spread in values is consistent with the expected statistical fluctuation. Recalling that the Ruderman effect, if present, would raise the frequency of pure water, relative to NaOH solutions, by ~ 15 ppm, we see that the frequency of the pure water signal is in fact 1.6 ppm lower, which is consistent with being the same within the statistical error of 2.5 ppm. The Ruderman effect is not present, and this is the result anticipated from our discussion which indicated that μ^+ ions are not present.

The muonium atoms which thermalize are chang-

TABLE IV. Muon precession frequency, in terms of the proton frequency, for water and basic solutions, before applying any corrections. Average of digitron and HP counter results, with purely statistical error.

	H ₂ O	0.1 <i>N</i> NaOH	0.5 <i>N</i> NaOH
ω_μ/ω_p	3.183350 (8)	3.183351 (11)	3.183359 (10)

ing state so rapidly (the muons in muonium process at ~2000 MHz in 11-kG transverse field) that they have no chance to become part of a stable molecule before they effectively depolarize. Recent experiments²⁵ have demonstrated this conclusively. The muons which are in normal molecules and which give us the observed modulation signal are therefore only those which have taken part in hot-atom reactions before becoming thermalized. To find the chemical state of these muons we must use the results of hot-atom chemistry, specifically the tritium studies which are the only available ones with a hydrogen isotope.

Table V gives the yield of products from tritium hot-atom reactions in H₂O, CH₂F₂, and CH₂Cl₂. Also given are the chemical shift of ordinary protons in the various product molecules, relative to protons in water.²⁶ Table V includes our estimate for the fraction of the various muon-containing species in our materials. An interesting confirmation of the prediction, for water, that most of the polarized sample consists of muons in μ HO is

found in work on the slow depolarization of μ^+ by Mn⁺⁺ ions in MnCl₂ solution.²⁷ The temperature and concentration dependence of this depolarization by line broadening (which is caused by magnetic interaction with the paramagnetic ion) bears a striking resemblance to the well-studied temperature and concentration effects of proton NMR line broadening in MnCl₂ solutions. The unusual functional dependences observed are specific to H₂O (or μ HO) molecules, which form complexes with the Mn⁺⁺.

B. Chemical Shifts of the Muon

We assume that the structure of a molecule in which a muon replaces a proton is unchanged apart from the different zero-point energy. This is consistent with the Born-Oppenheimer analysis, which states that vibrational energies are of order $(M_e/M)^{1/2}$ compared to electronic energies; we have $(M_e/M)^{1/2} = 0.07$.²⁸ The muon zero-point energy is about three times that of the proton, so

TABLE V. Data used to estimate the muon chemical shift in water and methylene cyanide. (a) Products of hot tritium (T) in several media, and fraction of total tritium found. No hot-atom data are available for CH₂(CN)₂, so CH₂F₂ and CH₂Cl₂ are used as analogs. (b) Estimated composition of the products of hot (nondepolarizing) muonium reactions; measured chemical shifts of the protons in these products, expressed as ppm relative to protons in water. δ (muon) is the proton shift corrected for the mass effect as explained in the text. Average shifts: Water, -1.8 ± 2.0 ppm; CH₂(CN)₂, $+0.1 \pm 1.5$ ppm.

		"Hot" products identified		
Medium	Species	(a) Products of hot tritium Fraction	Remarks	
H ₂ O ^a	TH	0.1	Some THO probably from ordinary (not "hot") reactions.	
	THO	0.9		
CH ₂ F ₂ ^b	TH	0.20	TF or TCl is also expected as a hot product, but cannot be identified. Remaining T went into nonhot channels, presumably.	
	THCF ₂	0.06		
	TH ₂ CF	0.02		
	Free radicals	0.03		
CH ₂ Cl ₂ ^b	TH	0.19		
	THCCl ₂	0.03		
	TH ₂ CCl	0.02		
	Free radicals	0.05		
		(b) Products of hot muonium reactions and chemical shifts		
Medium	Species	Fraction	δ (proton) ^c	δ (muon)
Water and NaOH solution	μ HO	0.9	0	-2.0
	μ H	0.1	0.4	-0.2
	μ H ₂ O ⁺	≈ 0	-11	-15
Methylene cyanide	μ H	0.7	0.4	-0.2
	μ HC(CN) ₂	0.3	1.5	0.9
	μ H ₂ C(CN)	≈ 0	3.0	2.4
	μ CN	≈ 0	2.0	1.4

^a T. Kambara, R. M. White, and F. S. Rowland, J. Inorg. Nucl. Chem. **21**, 210 (1961).

^b R. A. Odum and R. Wolfgang, J. Am. Chem. Soc. **85**, 1050 (1963).

^c Reference 26.

that a muon bound to oxygen, for example, has ~ 0.45 eV more energy than the OH ground state. This will increase the bond distance, in the $O\mu$ system, because the internuclear potential is asymmetric. The amount of increase, and the consequent decrease in diamagnetic shielding, was estimated by Ruderman⁶ for the ionic case he considered, and by Breskman and Kanofsky²⁹ for some diatomic molecules. The latter treatment, when an algebraic error is corrected,³⁰ shows that the bond distance increase in OH, HCl, H_2 , and CH is ~ 0.03 Å. The decrease of shielding with distance was estimated for the first three bonds^{6,29,30} as 20 ppm per Å, so the muon will be less shielded than the corresponding proton of Table V by 0.6 ppm.

Liquid water presents a special complication: The shielding is less in liquid water than in the vapor phase by 4 ppm. This effect is ascribed to the hydrogen bonding which causes water to be partially associated in the liquid phase. The mechanism by which the shielding is changed has been considered by Pople and collaborators.³¹ The attraction of the proton to a neighboring oxygen has two effects: it increases the average OH distance, and it interferes directly with the shielding currents set up in an isolated molecule. Both these effects tend to reduce the shielding of the proton. When a muon is substituted for the proton, the former effect is enhanced, while the latter remains about the same. The "hydrogen bond" effect should be larger for a muon than a proton; as an upper limit, it might be doubled.³² We assume 4 ppm as the

limit of muon-proton difference in water, and assign for the difference 2 ± 2 ppm.

Table V shows the values for chemical shifts, δ , of protons in the various molecules that are expected to contain the muon; the muon-proton differences discussed above; and finally the weighted averages of the chemical shifts. To assign errors we must consider both the composition and the muon-proton difference uncertainties. From the table it is clear that for water a change in the assignment of hot-product fractions will not change the result by more than the 2 ppm which we have assigned for an error in the μ HO shift, so 2 ppm is assigned (in the sense of 1 standard deviation) for the uncertainty in the chemical-environment correction in H_2O (no distinction is necessary between H_2O and NaOH, the presence of the Na^+ and OH^- ions has an effect ≤ 0.1 ppm). For methylene cyanide the composition is the chief uncertainty, but fortunately all the reasonable candidates for the molecular fate of the muon have chemical shifts very similar to that of water (as, in fact, do most molecules). The unweighted rms deviation of the methylene cyanide δ values in column 5 is 1.4 ppm. We assign a standard deviation of 1.5 ppm.

VI. CORRECTIONS, ERRORS, AND RESULTS

We collect here the corrections, most of which have been discussed in the previous chapters. In Table VI we find the uncorrected frequency ratios. Since the pure water and NaOH solutions have the

TABLE VI. Uncorrected results for ω_μ/ω_p , corrections (expressed in parts per million of ω_μ/ω_p), and systematic-uncertainty assignments.

	Water		$CH_2(CN)_2$	
Digitron result	3.1833556(54)		3.1833385(70)	
HP Counter result	3.1833503(52)		3.1833419(65)	
Average ^a	3.1833529(64)		3.1833402(72)	
Effect	Correction (ppm)	Error (ppm)	Correction	Error
(a) Target-out contribution	-0.4	0.4	Same	
(b) Container-wall contribution	...	0.1	Same	
(c) Bulk susceptibility	+1.5	0.3	Same	
(d) Small magnetic effects	...	0.5	Same	
(e) Proton resonance frequency at magnet center	...	0.8	Same	
(f) Weighted average over field map	-0.3	1.0	Same	
(g) Chemical shift	-1.8	2.0	+0.1	1.5
Net corrections	-1.0		+0.9	
Corrected result ^a	3.1833497(76)		3.1833431(83)	
Final average ^a			3.1833467(82) (2.6 ppm)	

^a See text for error treatment.

same frequency, both as observed and as expected on physical grounds, they are combined into "all H₂O" data. Digitron and HP Counter data are shown separately. Errors in the ratios at this stage are statistical errors in the muon frequency ω_μ . In taking the average of digitron and HP results we increased the error by adding the square of the internal-consistency error, $\frac{1}{2}(\text{Dig-HP})^2$, to the square of the statistical error. Table VI also gives:

(a) The contribution with target out. This rate was 2.5% of the rate with target. The asymmetry was low ($A = 0.05$) but the frequency was definitely higher than that of the whole sample. We find a correction, to the frequency ratio, of -0.4 ppm and assign an uncertainty equal to correction.

(b) Container-wall contribution. This was 1% of the target-in rate. Chemistry and magnetic field are close to that of the target sample. Uncertainty 0.1 ppm.

(c) Bulk-susceptibility correction as explained in Sec. III C: 1.5 ppm; error assigned, 0.3 ppm.

(d) Small magnetic effects as discussed in Sec. III C (e.g., undetectably small magnetic materials in the probe); error assigned, 0.5 ppm.

(e) Proton resonance frequency at the center of the magnet; error assigned, 0.8 ppm.

(f) Weighted average over the field map (Table II). Correction -0.3 ppm; error assigned, 1 ppm.

(g) Chemical shift as discussed in Sec. V. Water: Correction -1.8 ppm, error 2 ppm; CH₂(CN)₂: correction $+0.1$ ppm, error 1.5 ppm.

To compare and combine results from the two different chemical systems it is appropriate to combine the purely statistical error with those other uncertainties which are essentially uncorrelated between the two sets of data: the central resonance frequency (e) and the weighted average (f). When this is done we get the "corrected result" line in Table VI, with the water ratio 3.1833497(76) and the methylene cyanide ratio 3.1833431(83). These are clearly consistent.

Finally, we take the weighted average of these uncorrelated results, and add to the error, in quadrature, the other errors from Table VI.³³ This results in the final answer, $\mu_\mu/\mu_p = 3.1833467(82)$ (2.6 ppm). Rounded off, this agrees with our previously published result,¹ with slightly smaller error.

VII. CONCLUDING REMARKS

A. Other Measurements

Table VII lists the other measurements^{34,35} of the muon magnetic moment. There is no disagreement within the larger errors of those measurements. The Princeton-Penn result is quoted with

TABLE VII. Published values of the magnetic moment of the muon expressed as ratio to the proton moment, μ_μ/μ_p .

Columbia (1963) ^a	3.18338(4) (13 ppm)
Berkeley (1963) ^b	3.18336(7) (22 ppm)
Princeton-Penn (1970) ^c	3.183369(24) (7.5 ppm)
Chicago (1970) ^d	3.183337(13) (4.1 ppm)
Present measurement	3.1833467(82) (2.6 ppm)

^a Reference 4.

^b Reference 5.

^c Reference 34. Chemical shift correction and uncertainty not included.

^d Reference 35. A systematic pressure-shift uncertainty has not been included in this error. See Ref. 35a.

no chemical-shift correction or related uncertainty. The Chicago result is preliminary in the sense that a theoretical 11-ppm correction has been applied for pressure effect, but no estimate is yet available on the uncertainty in that correction.^{35a}

B. Mass of the Muon

The g factors of the muon and electron are extremely well known; the ratio of the proton moment to the electron moment is known to about 0.2 ppm.⁷ Therefore we can form $m_\mu/m_e = (g_\mu/g_e) \times (\mu_p/\mu_\mu)(\mu_e/\mu_p)$. The result is $m_\mu/m_e = 206.7682(5)$. Using⁷ $m_e = 0.5110041(16)$ MeV we find $m_\mu = 105.6594(4)$ MeV. This is 5 ppm lower than the value in the 1971 Particle Data Group³⁶ table, which had a 13-ppm error assignment.

C. Muonium Hyperfine Interval and the Fine-Structure Constant

As pointed out in the Introduction, Eq. (1), the muon moment, the fine-structure constant, and the muonium hyperfine interval ν_M are related by a theoretical expression whose radiative corrections were thought to be reliable at the part-per-million level. Recently³⁷ a new radiative-recoil term was calculated which made a difference of 5.6 ppm, but presumably this will be the last of such surprises. New and accurate values for ν_M have recently become available: The Chicago group reports $\nu_M = 4463.3022(89)$ MHz in their high-field work,³⁵ and very recently³⁸ finds 4463.3013(40) MHz by a low-field technique. The Yale group³⁹ finds 4463.311(12) MHz. The average of these consistent results is 4463.3023(35) MHz. Using the theoretical evaluation of Eq. (1) given by Fulton, Owen, and Repko³⁷ with our muon-moment value and this value for ν_M we get for the fine-structure constant

$$\alpha^{-1} = 137.03632(19) \text{ (1.4 ppm)}. \quad (5)$$

The error is one-half the root sum square of 2.6 ppm for μ_μ/μ_p , 0.8 ppm for ν_M , and a theoretical uncertainty of 0.6 ppm estimated by Brodsky and Erickson⁴⁰ for uncalculated radiative terms in Eq. (1). This result is to be compared with the recommended value,

$$\alpha^{-1} = 137.03602(21) \text{ (1.5 ppm)} \quad (6)$$

given by Taylor, Parker, and Langenberg.⁷ The value of Eq. (6) depends primarily on the ac Josephson effect determination of $2e/h$,⁴¹ the gyromagnetic ratio of the proton, $\gamma_p \equiv \omega_p/B$, and to a lesser extent the value of α obtainable from the hydrogen hyperfine interval and some theoretical argument about proton structure; it has no input from muonium, and can therefore be compared directly with Eq. (5). The difference is 2.2 ppm, and the error in the difference is 2.1 ppm, so agreement is satisfactory at this level of accuracy. The agreement is particularly gratifying in view of the long-standing difficulty with the erroneous value of α derived from the 1964 muonium result^{48,39} and the Columbia value for μ_μ/μ_p . Preliminary results of a new measurement of γ_p at the National Bureau of Standards⁴² indicate that the value in Eq. (6) will be superseded by a slightly smaller value, with smaller error. However, there will still be no statistically significant discrepancy.

D. Other Consequences of the New Value of μ_μ/μ_p

(1) $a \equiv \frac{1}{2}(g-2)$ of the muon. The observed quantity in the "g-2" experiment is the ratio of the g-2 frequency to the proton resonance frequency in the same field, ω_{g-2}/ω_p . The anomaly is then obtained as

$$a = (\omega_{g-2}/\omega_p) / [(\mu_\mu/\mu_p) - (\omega_{g-2}/\omega_p)],$$

so the value of a , and its error, depend directly on μ_μ/μ_p . However, the current best value for a

has an error of 270 ppm,² so the new value for μ_μ/μ_p makes no significant difference. Work has begun at CERN³ looking toward a far more accurate g-2 measurement.

(2) Muonic x rays. Energy levels in muonic x rays are directly proportional to the muon mass. Recently muonic x ray measurements to ~50 ppm accuracy have been reported.⁴³ The increase in accuracy of the muon mass eliminates a nonnegligible uncertainty in the level calculations, although the 5-ppm decrease in the muon mass value is insignificant compared to the discrepancies reported in Ref. 43.

(3) Muon neutrino mass. The charged-pion mass, muon mass, and muon momentum in $\pi-\mu$ decay can be combined to put a limit on the muon neutrino mass m_ν . A recent improved value of the pion mass has been used,⁴⁴ with the old muon mass, to put a limit of ~0.6 MeV on m_ν . However, this limit is still dominated by the pion mass error, 0.008 MeV, so that the new muon mass will play no part until the pion mass error is further reduced.

ACKNOWLEDGMENTS

M. Delay and J. Justice assisted in various aspects of the experiment. Two of the authors (D. L. Williams and R. W. Williams) owe special thanks to members of the CERN Muon Storage Ring group and Electronics group for help during the formative stages of the experiment.

We are grateful to various experts for advice on chemical questions, especially Professor L. Slutsky and Professor J. A. Pople. Dr. B. N. Taylor provided helpful advice on the fundamental constants. Technical assistance from many people at LBL was invaluable, and is gratefully acknowledged. We thank James Vale and the 184-in. Cyclotron crew for excellent cooperation in running the experiment.

*Work supported by the National Science Foundation and the U. S. Atomic Energy Commission.

†Present address: 9 Heron's Place, Marlow, Bucks, England.

‡Present address: 1. Physikalisches Institute, University of Heidelberg, Germany.

¹J. F. Hague, J. E. Rothberg, A. Schenck, D. L. Williams, R. W. Williams, K. K. Young, and K. M. Crowe, *Phys. Rev. Letters* **25**, 628 (1970).

²J. Bailey, W. Bartl, G. von Bochman, R. C. A. Brown, F. J. M. Farley, H. Jostlein, E. Picasso, and R. W. Williams, *Phys. Letters* **28B**, 287 (1968).

³E. Picasso (private communication). See also the CERN proposal by E. Picasso and co-workers, CERN

Report No. PH I/COM-69/20, 1969 (unpublished).

⁴D. P. Hutchinson, J. Menes, G. Shapiro, and A. M. Patlach, *Phys. Rev.* **131**, 1351 (1963). This paper contains references to previous work.

⁵G. McD. Bingham, *Nuovo Cimento* **27**, 1352 (1963).

⁶M. A. Ruderman, *Phys. Rev. Letters* **17**, 794 (1966).

⁷B. N. Taylor, W. H. Parker, and D. N. Langenberg, *Rev. Mod. Phys.* **41**, 375 (1969). We follow their notation where possible. Numerically, we use their "recommended" values except that for μ_p/μ_B we use the results of P. F. Winkler, D. Kleppner, M. T. Myint, and F. G. Walther, *Phys. Rev. A* **5**, 83 (1972).

⁸W. E. Cleland, J. M. Bailey, M. Eckhause, V. W. Hughes, R. M. Mobley, R. Prepost, and J. E. Rothberg,

Phys. Rev. Letters **13**, 202 (1964).

⁹R. W. Williams and D. L. Williams, Phys. Rev. D (to be published).

¹⁰R. A. Swanson (private communication). G. R. Henry and G. Schrank, LRL Report No. UCRL-11086, 1963 (unpublished).

¹¹Logic notation used is (a) a *dot* implies a logical "and"; (b) a *plus* implies a logical "or."

¹²The asymmetry *A* was significantly higher with the system which had least count of 0.5 nsec than with the system of least count 1.25 nsec.

¹³R. A. Swanson, Rev. Sci. Instr. **31**, 149 (1960).

¹⁴Kai L. Lee, LBL Report UCID No. 3467, 1970 (unpublished).

¹⁵Without this latter precaution the probability of stopping the scaler at a given time interval can depend on whether the first scalar stage is at 1 or 0, which in turn can cause a bias in favor of odd (or even) numbers. We have checked with Monte Carlo data that such an odd-even effect cannot lead to an error in the frequency measurement.

¹⁶G. McD. Bingham, Lawrence Radiation Laboratory Report No. UCRL-10107, 1963 (unpublished).

¹⁷This was not possible for the HP counter because the long delay-line introduced a slow shift in phase from day to day.

¹⁸Taylor, Parker, and Langenberg, Ref. 7, use the notation μ'_b to refer to the combination $[1 - \sigma(\text{H}_2\text{O})]\mu_b$ which occurs in many measurements. This notation is of no utility to us, since σ for the muon is different from that for the proton.

¹⁹S. K. Allison and M. Garcia-Munoz, in *Atomic and Molecular Processes*, edited by D. R. Bates (Academic, New York, 1962), Chap. 19.

²⁰Vernon W. Hughes, Ann. Rev. of Nucl. Sci. **16**, 445 (1966).

²¹R. Wolfgang, Progr. Reaction Kinetics **3**, 99 (1965).

²²K. Applegate, L. J. Slutsky, and R. C. Parker, J. Am. Chem. Soc. **90**, 6909 (1968).

²³We are indebted to Professor Y. Pocker for advice on the chemistry of this compound.

²⁴Several of the water runs were done with deoxygenated water; one was with water at 80 °C. There was no difference outside statistics between these and the regular distilled water.

²⁵J. H. Brewer, K. M. Crowe, R. F. Johnson, A. Schenck, and R. W. Williams, Phys. Rev. Letters **27**, 297 (1971). In this study we show that the addition of a few mole percent of a fast-reacting substance, such as I₂, catches the muonium atoms before the muons can depolarize.

²⁶Chemical shifts are tabulated, for example, in J. W. Emsley, T. Feeney, and L. H. Sutcliffe, *High Resolution Nuclear Magnetic Resonance Spectroscopy* (Pergamon Press, Oxford, England, 1965).

²⁷A. Schenck (private communication). See also A. Schenck, Phys. Letters **32A**, 19 (1970).

²⁸An example of the insensitivity of structure to mass change is the bond angle in water. For H₂O it is 104.523°, for HDO it is 104.529°, and for D₂O, 104.474°.

²⁹D. Breskman and A. Kanofsky, Phys. Letters **33B**, 309 (1970).

³⁰R. W. Williams, Phys. Letters **34B**, 63 (1971). This note corrects the error originally made by T. W. Marshall, Mol. Phys. **IV**, 61 (1962). For H₂ we use Marshall's calculation of the change of shielding with bond distance.

³¹J. A. Pople, W. G. Schneider, and H. J. Bernstein, *High-resolution Nuclear Magnetic Resonance* (McGraw-Hill, New York, 1959).

³²We are indebted to Professor J. A. Pople for advice on this matter.

³³We took the chemical error to be the average of the two, 1.75 ppm. Various other weighting methods lead to the same result. If all errors were assumed to be uncorrelated the final error would be 2.1 ppm.

³⁴D. P. Hutchinson, F. L. Larsen, N. C. Schoen, D. I. Sober, and A. S. Kanofsky, Phys. Rev. Letters **24**, 1254 (1970).

³⁵R. De Voe, P. M. McIntyre, A. Magnon, D. Y. Stowell, R. A. Swanson, V. L. Telegdi, Phys. Rev. Letters **25**, 1779 (1970); **26**, 213(E) (1971).

^{35a}*Added in proof.* The theoretical pressure-shift correction has now been published: J. Jarecki and R. M. Herman, Phys. Rev. Letters **28**, 199 (1972). The result is a correction of -7.8 ± 2.3 ppm, changing the Chicago result for μ_μ/μ_b to 3.183 349(15).

³⁶Particle Data Group, Rev. Mod. Phys. **43**, S1 (1971).

³⁷T. Fulton, D. A. Owen, and W. W. Repko, Phys. Rev. Letters **26**, 61 (1971). The value for ν_M given in Ref. 1 does not contain this correction.

³⁸D. Favart, P. M. McIntyre, D. Y. Stowell, V. L. Telegdi, R. De Voe, and R. A. Swanson, Phys. Rev. Letters **27**, 1336 (1971).

³⁹T. Crane, D. Casperson, P. Crane, P. Egan, V. W. Hughes, R. Stambaugh, P. A. Thompson, and G. zu Putlitz, Phys. Rev. Letters **27**, 474 (1971). This paper points out a quadratic term in the pressure shift, which accounts in part for the discrepancy in the early high-field measurement, Ref. 8.

⁴⁰S. J. Brodsky and G. W. Erickson, Phys. Rev. **148**, 26 (1966).

⁴¹T. F. Finnegan, A. Denenstein, and D. N. Langenberg, Phys. Rev. B **4**, 1487 (1971).

⁴²P. T. Olsen and R. L. Driscoll, contribution to the Teddington International Conference on Atomic Masses and Related Fundamental Constants, Teddington, England, 1971 (unpublished).

⁴³M. S. Dixit, H. L. Anderson, C. K. Hargrove, R. J. McKee, D. Kessler, H. Mes, and A. C. Thompson, Phys. Rev. Letters **27**, 878 (1971).

⁴⁴G. Backenstoss, H. Daniel, K. Jentsch, H. Koch, H. P. Hovel, F. Schmeissner, K. Springer, and R. L. Stearns, Phys. Letters **36B**, 403 (1971).